

Reactive epitaxy of metallic hafnium silicide nanocrystals

G. A. Fiorentini, Marina S. Leite, V. L. Pimentel, L. A. Montoro, A. J. Ramirez, and G. Medeiros-Ribeiro^{a)}

Laboratório Nacional de Luz Síncrotron, Caixa Postal 6192-CEP 13084-971, Campinas, Sao Paulo 13084-971 Brazil

(Received 10 April 2008; accepted 17 June 2008; published online 8 July 2008)

Hafnium silicide islanding occurs spontaneously when metallic Hf is deposited on a Si(001) surface and subsequently annealed at 750 °C. Different coverages were investigated by scanning tunneling microscopy (STM) in order to verify distinct stages of island formation. Small islands occurred for 0.26 ML of deposited Hf, coalescing into flat top islands for longer deposition times. Atomic resolution STM and nanobeam electron diffraction allowed the determination of the mature islands top face structure, identified as the (061) surface of the HfSi₂ in the C49 phase. Finally, scanning tunneling spectroscopy was carried out over the smallest islands, demonstrating their metallic behavior. © 2008 American Institute of Physics. [DOI: 10.1063/1.2956665]

Hafnium dioxide (HfO₂) exhibits a large relative permittivity (high- κ) when compared to SiO₂, which is one of the key parameters required for the continuous miniaturization of semiconductor devices.¹ Since SiO₂ is still present at the semiconductor-insulator interface even for Hf based electronics, a great effort is needed for the understanding of this system from the materials and electronics stand point. The stability of HfO₂ onto SiO₂ has been discussed from a theoretical and experimental perspective,² where it was found from density functional theory calculations that the formation of Hf silicides on SiO₂ is not thermodynamically favored with respect to Hf silicate. Yet, recent experimental reports demonstrating silicide formation on stacked structures of HfO₂/SiO₂ upon annealing at 750 °C,³ and silicide formation in oxygen deficient conditions,^{4,5} reveal that silicides can be formed during typical semiconductor processing steps. Also noteworthy is a scanning tunneling microscopy (STM) report on the degradation of Hf silicate into HfSi_x.⁶ These results highlight the importance of the elucidation of the structural and electronic properties of small HfSi_x crystallites, as they can severely impact the performance of field effect transistors.

Previously, HfSi_x islands formed in the Volmer–Weber growth mode were investigated by atomic force microscopy, low energy electron diffraction (LEED) and x-ray photoemission spectroscopy (XPS).⁷ Later, a subsequent report using LEED, XPS, and x-ray photoelectron diffraction (XPD) suggested an ordered surface.⁸ XPD and concurrent simulation utilizing a C49 structural model were in good agreement.⁸ However, a clear identification of the crystalline structure is still lacking.

Here we carry out detailed investigations of HfSi_x islands in different stages of formation using nanobeam electron diffraction (NBD) and ultrahigh vacuum (UHV)-STM. We find that by increasing Hf coverage, the nanocrystal evolution proceeds through coalescence and growth processes leading to flat top HfSi₂ islands with rearranged (061) facets. Finally, we probe the electronic properties of small islands utilizing scanning tunneling spectroscopy (STS), demonstrating metallic behavior for islands as small as 5 nm.

The samples investigated in this work were grown in a homemade molecular beam epitaxy (MBE) system with a base pressure of 4×10^{-11} Torr, which is coupled to a VT-UHV Omicron STM to allow *in situ* characterization. Boron doped Si(001) substrates were cleaned under an Argon (Ar) plasma for 30 s in a load-lock chamber, prior to introduction in the UHV-MBE system. Flash annealing steps at 1200 °C for 30 s through a direct heating current were conducted until an oxide-free surface was obtained. During the annealing, the temperature was monitored by an infrared pyrometer and the pressure was maintained below 1×10^{-10} Torr. Afterward, three different samples were grown at room temperature using an electron beam Hf evaporation source, calibrated to a deposition rate of 1.4 ML/min, resulting in coverages of 0.3 ML for sample A, 0.7 ML for sample B, and 1.4 ML for sample C. All samples were annealed at 750 °C for 10 s after Hf deposition in order to allow the reaction between Hf and Si.³ They were subsequently studied with STM and STS. The temperature was chosen to be close to typical semiconductor processing conditions.³ Unannealed samples revealed a smooth surface, with a disordered layer of Hf adatoms. NBD specimens were prepared in a plan view mode through manual and dimpler polishing, and Ar⁺ ion-beam thinning using a Gatan precision ion polishing system. The NBD experiments were performed using a JEM 3010 URP transmission electron microscope operated at 300 kV with a 5 nm probe size.

Figures 1(a) and 1(b) show STM images taken on samples A and C. For all samples, Volmer–Weber islands oriented along the $\langle 110 \rangle$ directions of the Si substrate were found. From the deposition sequence, one finds a coalescence process, starting from sample A, with a high density of small islands [Fig. 1(a)], ending up with coalesced islands with an average size of 50 nm, 1–2 nm in height, and an areal coverage of 70% (sample C). In Fig. 1(b), the coalescence region between two large islands is indicated by an arrow, where their atomic structure lines up.

The coalescence and growth processes observed on samples B (not shown) and C can be observed at their initial stages on sample A. Figure 2 shows the island size evolution. Figure 2(a) shows a primitive island, about 4 nm in length and 0.5 nm in height. The periodicity of the top atoms is 0.384 ± 0.005 and 0.477 ± 0.005 nm along the Si substrate

^{a)} Author to whom correspondence should be addressed. Electronic mail: gmedeiros@lnls.br.

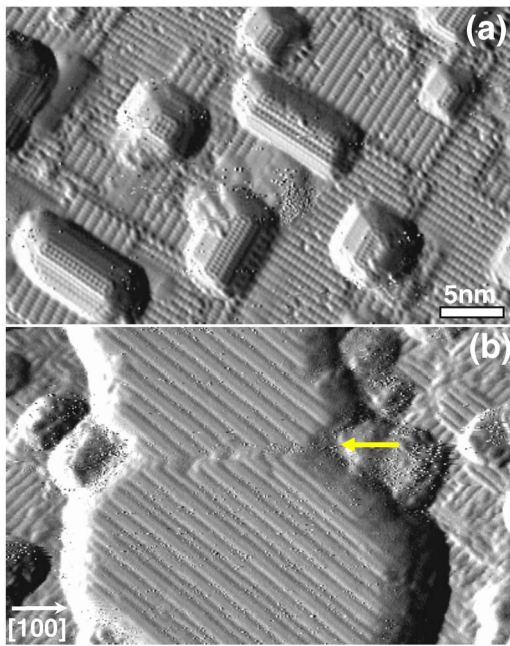


FIG. 1. (Color online) $25 \times 40 \text{ nm}^2$ STM scans of HfSi_x islands obtained by reactive epitaxy after the deposition of (a) 0.26 ML and (b) 1.38 ML of Hf. (b) shows one mature island in a coalescence process. Both samples were subsequently annealed for 10 s at $750 \text{ }^\circ\text{C}$ after Hf deposition. The grayscale is associated with the height derivative along the slow scan direction. $V_{\text{tip}} = -2.0$ and $+1.6 \text{ V}$ for images (a) and (b).

$[\bar{1}10]$ and $[110]$ directions, not characteristic of any Hf silicide compound known.⁹ Nevertheless, the island atom spacing along the $[\bar{1}10]$ direction matches the Si lattice parameter. Figure 2(b) presents a coalescence between two primitive islands, leading to a transitional structure. The periodicity along the $[110]$ direction is $0.391 \pm 0.005 \text{ nm}$, whereas along $[110]$ an order is not clearly established. In Fig. 2(c), an elongated island in its later stage of growth is shown, with twice the length of the primitive islands and the same width. These images show that HfSi_x islands size evolution can occur by a coalescence process or by growth along the $\langle 110 \rangle$ directions.

At this point, the crystal structure as well as the stoichiometry are not clearly identified, and these preliminary stages are precursors to more stable phases. The mature islands from sample C, on the other hand, present a very well defined periodic structure, which can be unequivocally ascribed to the C49 phase of the HfSi_2 , as it will be shown ahead. Figure 3 exhibits atomic resolution images on a typical flat top island, oriented with respect to the substrate. Figure 3(a) shows the island top surface, with alternating row

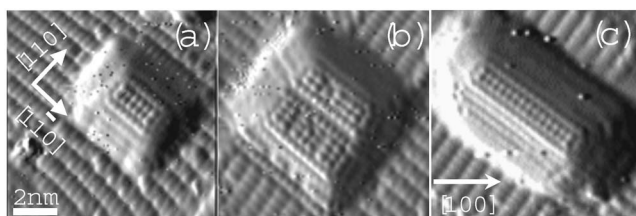


FIG. 2. $10 \times 10 \text{ nm}^2$ atomic resolution STM images on sample A: (a) a primitive island, (b) a transitional island, and (c) an elongated, noncoalesced island. Note that the transitional island is formed by the coalescence of two primitive islands. The grayscale of the images is associated with the height derivative along the slow scan direction. $V_{\text{tip}} = -2.0 \text{ V}$.

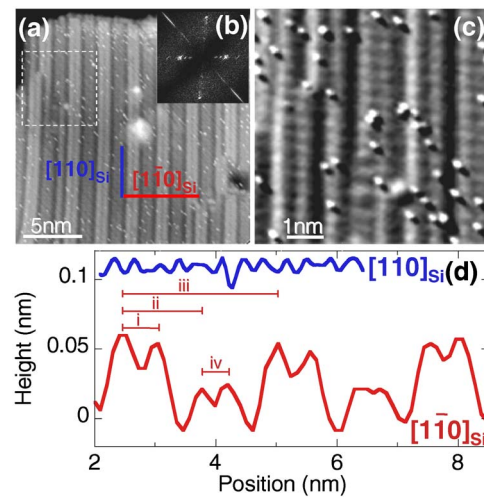


FIG. 3. (Color online) (a) $20 \times 20 \text{ nm}^2$ STM scan of a HfSi_2 mature island of sample C. The gray scale is keyed to the height. (b) Power spectrum of the image shown in (a). (c) $6.5 \times 6.5 \text{ nm}^2$ STM scan of the selected area in (a). The gray scale corresponds to the height derivative along the substrate $[100]$ direction. (d) Line scans taken along $[110]_{\text{Si}}$ (blue) and $[\bar{1}10]_{\text{Si}}$ (red) directions, showing the periodicity of the atoms. $V_{\text{tip}} = +1.6 \text{ V}$.

pairs with different heights. A two-dimensional power spectrum of this image is shown in Fig. 3(b). Along the Si substrate $[110]$ direction ($[110]_{\text{Si}}$), one finds a short period structure, whereas along the $[\bar{1}10]_{\text{Si}}$, three spots are shown. Figure 3(c) is a magnified view of the region indicated by the dashed square in Fig. 3(a). Except for a few regions (upper left corner), the row pairs run continuously across the island. Figure 3(d) presents two line scans aligned with the $[110]_{\text{Si}}$ (blue) and $[\bar{1}10]_{\text{Si}}$ (red) directions taken on the image shown in Fig. 3(a), color coded accordingly. The average spacing along the $[110]_{\text{Si}}$ direction was measured and resulted in $0.354 \pm 0.005 \text{ nm}$, using the Si substrate lattice spacing as a reference. Along the $[\bar{1}10]_{\text{Si}}$ direction, the interatomic distances were found to be $i=0.510 \text{ nm}$, $ii=1.310 \text{ nm}$, $iii=2.550 \text{ nm}$, and $iv=0.420 \text{ nm}$. The error is $\pm 0.005 \text{ nm}$ for all measurements. The row pairs can be seen with a height difference of about 0.2 \AA .

By using only the surface periodicities inferred from the STM measurements, it is extremely hard to identify the crystalline structure of the islands. We thus use NBD to make a precise assignment of the island structure and its orientation. Figure 4(a) shows an electron diffraction pattern obtained in the $[013]$ zone axis for a mature island in sample C. The diffraction pattern was confirmed by simulation utilizing HfSi_2 in the C49 structure,¹⁰ corroborating the suggestion by Siervo *et al.*⁸ Figure 4(b) shows the corresponding (061) surface of the crystallite which is to be compared to Fig. 3. The only deviation from this model concern the Si–Hf pair row (indicated by the bars on the top side of the image), in which the Hf atom row alternates with the Si atom row in the unreconstructed surface. The atom spacing inferred from the STM images suggest a rearrangement of the Si–Hf atoms in a single row. Lastly, the periodicities along the $[110]_{\text{Si}}$ obtained from the simulation for the Si and Si–Hf atom rows indicated by braces ($i=iv=0.420 \text{ nm}$, $ii=1.310 \text{ nm}$, and $iii=2.580 \text{ nm}$) (Ref. 10) are consistent with the STM measurements. Figure 4(c) shows a perspective view of the structural model with the HfSi_2 unit cell represented schematically.

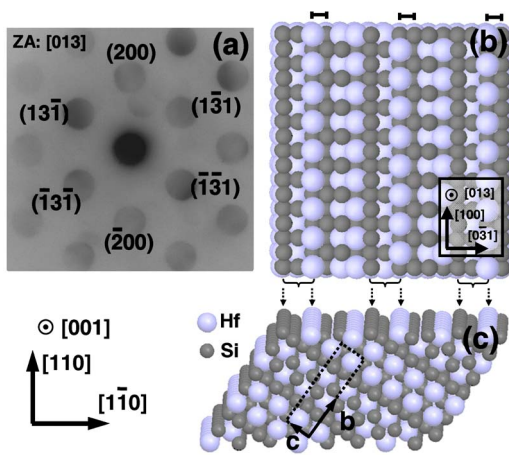


FIG. 4. (Color online) (a) Nanobeam electron diffraction measured over the islands of sample C. (b) Structural model (Ref. 10) of the unreconstructed surface indicating the Si–Hf pairs (see braces) shown on the line scan of Fig. 3(d). The bars indicate where Si atoms would be rearranged and aligned to the Hf atoms, to account for the STM observations. (c) Perspective view of the structural model showing the orthorhombic unit cell. The directions shown on the left refer to the substrate orientation.

Finally, the electronic properties of the HfSi_x islands were evaluated using STS. In Figs. 5(a) and 5(b), the topography and associated current map, measured at $V_{\text{tip}} = -1.47$ V, are shown. Figures 5(c) and 5(d) show the IV and dI/dV curves for two representative islands [(1) and (2)] and the Si substrate, taken as a reference. Figure 5(b) shows an excess current through the islands, indicating a higher density of states. This can be seen as well from the IV characteristics shown in Fig. 5(c). A finite conductance at 0 V for both islands [Fig. 5(d)] demonstrates the metallic behavior of the HfSi_x crystalline nanostructures.

Summarizing, Hf silicide Volmer–Weber islands can be spontaneously formed by the deposition of metallic Hf on a Si(001) substrate at room temperature and a subsequent annealing at 750 °C for 10 s. By increasing Hf coverage, STM examination showed that the primitive islands can develop through a coalescence process or by growth along the $\langle 110 \rangle$ directions, leading to a mature structure with a stable crystalline phase. NBD measurements and simulation (not shown) revealed a (061) surface of the C49 phase of HfSi_2 for these structures. STS measurements on islands as small as 4 nm in lateral size exhibited a metallic behavior, indicated by their local conductance. Therefore, care must be exercised in providing stack structures resilient to silicide formation during semiconductor processing steps.

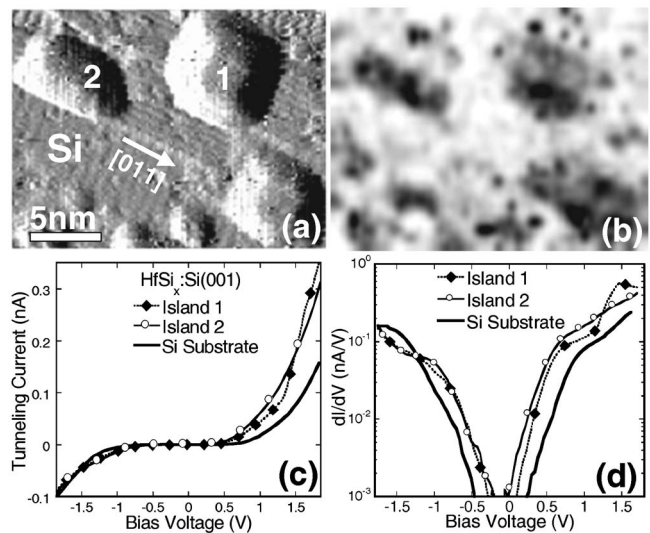


FIG. 5. (a) 22×17 nm² STM scan of the topography of sample A. The grayscale is associated with the height derivative along the slow scan direction. $V_{\text{tip}} = -2.0$ V. (b) Spectroscopic image of the same area shown in (a). The grayscale is associated with the current intensity for an applied bias of $V_{\text{tip}} = -1.47$ V. (c) IV curves measured above the substrate and two representative islands showing the metallic behavior of the HfSi_x 3D structures. (d) Differential conductance curves showing the metallic behavior of the islands compared to the Si substrate.

The authors acknowledge financial support from CNPq (SPMBrazil network) and FAPESP Contract No. 2007/05165-7.

¹International Technology Roadmap for Semiconductors (<http://www.itrs.net/>).

²M. Gutowski, J. E. Jaffe, C.-L. Liu, M. Stoker, R. I. Hedge, R. S. Rai, and P. J. Tobin, *Appl. Phys. Lett.* **80**, 1897 (2002).

³H. Takahashi, J. Okabayashi, S. Toyoda, H. Kumigashira, M. Oshima, K. Ikeda, G. L. Liu, Z. Liu, and K. Usuda, *J. Appl. Phys.* **99**, 113710 (2006).

⁴D.-Y. Cho, K.-S. Park, B.-H. Choi, S.-J. Oh, Y. J. Chang, D. H. Kim, T. W. Noh, R. Jung, J.-C. Lee, and S. D. Bu, *Appl. Phys. Lett.* **86**, 041913 (2005).

⁵R. Jian, E. Xie, and Z. Wang, *Appl. Phys. Lett.* **89**, 142907 (2006).

⁶J.-H. Lee and M. Ichikawa, *J. Vac. Sci. Technol. A* **20**, 1824 (2002).

⁷H. T. Johnson-Steigleman, A. V. Brinck, S. S. Parihar, and P. F. Lyman, *Phys. Rev. B* **69**, 235322 (2004).

⁸A. de Siervo, C. R. Flüchter, D. Weier, M. Schürmann, S. Dreiner, C. Westphal, M. F. Carazzolle, A. Pancotti, R. Landers, and G. G. Kleiman, *Phys. Rev. B* **74**, 075319 (2006).

⁹W. Ng, W. McMurdie, H. Paretzkin, B. Hubbard, and C. Dragoo, NBS, ICDD Grant in Aid (1987).

¹⁰Simulations were obtained using JEMS (Java Electron Microscopy Software), P. A. Stadlmann, *Ultramicroscopy* **21**, 131 (1987).